



OPEN

An empirical evaluation of fuzzy bidirectional long short-term memory with soft computing based decision-making model for predicting volatility of cryptocurrencies

Mahmoud Ragab^{1,2}✉

Cryptocurrencies have received a lot of attention from central banks, investors, and governments worldwide. The insufficiency of any method of political guideline and their market is far from "effective", so they want novel regulation methods shortly. From an econometric perspective, the technique underlying the growth of the cryptocurrencies' volatility was observed to demonstrate similarities and differences with other economic time series, e.g., foreign exchange yields. Accurate prediction of cryptocurrency price fluctuations is significant for effectual portfolio management and improves economic models by identifying potential risks and attacks. With the growing use of AI in various fields, its application in financial markets, especially cryptocurrencies and stocks, is an emerging research area. This study presents an Empirical Evaluation of Fuzzy Bidirectional Long Short-Term Memory with a Soft Computing-based Decision-Making Model for Predicting Volatility of Cryptocurrencies (FBLSTMSC-DMPVC) technique. The primary focus of the FBLSTMSC-DMPVC technique is to present a robust and intelligent framework for an advanced decision-making model to predict cryptocurrency volatility. Initially, the presented FBLSTMSC-DMPVC method performs the data preprocessing process using Z-score normalization to ensure all features are standardized and scaled. Furthermore, the fuzzy bidirectional long short-term memory (FBLSTM) method predicts cryptocurrency volatility. To enhance the hyperparameters of the FBLSTM technique, the improved carnivorous plant algorithm (ICPA) is employed. A wide range of simulation is accomplished to ensure the impact of the FBLSTMSC-DMPVC technique. The FBLSTMSC-DMPVC technique portrayed a superior MAPE value of 0.7939 for BTC, 0.8633 for ETH, 0.6187 for LTC, and 0.6667 for XRP, demonstrating its performance across various cryptocurrencies.

Keywords Cryptocurrencies, Volatility, Soft computing, Decision making, Artificial intelligence, Fuzzy model

The financial markets eventually presented several new technologies, but these mainstream have not succeeded or survived. However, the occurrence of cryptocurrencies has attracted several investigators' attention worldwide, and various investigators have predicted these digital currencies would have destructive consequences on the economic system¹. Cryptocurrencies are technologies with unpredicted behaviour that are complex to forecast regarding their future acceptance in the worldwide financial system. Cryptocurrencies have involved the interest of several investors, and it has become another form of coin owing to their digital features². The digital attributes have made cryptocurrencies more dynamic than classical currencies in payment cases because these depend on cryptographic proof. In measurable finance, instability denotes the conditional standard variance or deviation of the fundamental assets that are proceeded³. Amongst several economic markets, the fast development of

¹Information Technology Department, Faculty of Computing and Information Technology, King Abdulaziz University, 21589 Jeddah, Saudi Arabia. ²Department of Mathematics, Faculty of Science, Al-Azhar University, Naser City, Cairo 11884, Egypt. ✉email: mragab@kau.edu.sa

the cryptocurrency market, its higher instability, and its applications in diverse business transactions have attracted the attention of investors and academics⁴. From a financial econometric viewpoint, this work is unstable in predicting typically and contains Autoregressive Conditional Heteroskedasticity (ARCH) and their generality, such as GARCH-form methods. Such time series methods using heteroscedastic errors are valid for modelling volatile economic market data. Like other financial time series, cryptocurrencies are forecasting, and heteroscedastic instability is an essential variable in risk management, which is a challenging task⁵.

The unpredictability of economic time series has gathered substantial attention from both practitioners and researchers, comprising risk managers, policymakers, and investors. These problems' significance is due to the wide variety of real-world applications in investment, option pricing, portfolio optimization, and risk management⁶. But, the unpredictability of economic series, because of its particular properties, is not a trivial challenge⁷. Such characteristics as an extended to sound sharing of multiple outliers, price fluctuations, the substantial impact of market microstructure, the conditional heteroscedasticity proceeds, and the occurrence of diverse time scales of stakeholders cause further progressive approaches to have complexities for higher predicting accurateness. Statistical analysis methods like multiple-linear regression are well-known, and amongst the others, the Integrated Moving Average (ARIMA) approach is generally utilized to forecast the data variable tendencies⁸. This method is used frequently to predict time series that are trend stationary, and it is not standard for weak stationary or non-stationary data. Also, statistical approaches, such as Deep Learning (DL) and Machine Learning (ML) methods, are utilized to forecast time series concerns⁹. The time series properties are often complex and non-linear, making it complex for these approaches to take the actual dynamics. Thus, some advanced ML methods have been implemented to address these tasks. Amongst DL methods, long short-term memory (LSTM) is a significant framework with time-series data¹⁰. Because LSTMs can remember and process components in time series data and forecast dependencies between data effectively. Cryptocurrencies' swift growth and volatility have created significant challenges in predicting their future behaviour, making them an intriguing research subject. Accurately forecasting cryptocurrency volatility is crucial for investors and policymakers to navigate complex and dynamic market conditions.

This study presents an Empirical Evaluation of Fuzzy Bidirectional Long Short-Term Memory with a Soft Computing-based Decision-Making Model for Predicting Volatility of Cryptocurrencies (FBLSTMSC-DMPVC) technique. The primary focus of the FBLSTMSC-DMPVC technique is to present a robust and intelligent framework for an advanced decision-making model to predict cryptocurrency volatility. Initially, the presented FBLSTMSC-DMPVC method performs the data preprocessing process using Z-score normalization to ensure all features are standardized and scaled. Furthermore, the fuzzy bidirectional long short-term memory (FBLSTM) method predicts cryptocurrency volatility. To enhance the hyperparameters of the FBLSTM technique, the improved carnivorous plant algorithm (ICPA) is employed. A wide range of simulation is accomplished to ensure the impact of the FBLSTMSC-DMPVC technique. The key contribution of the FBLSTMSC-DMPVC technique is listed below.

- The Z-score normalization standardizes the data by transforming it into a standard scale, ensuring that each feature contributes equally to the model. This process mitigates the impact of scale-related biases, resulting in more accurate predictions. It improves model performance by improving consistency across features and making them comparable.
- The FBLSTM method effectively handles complex, non-linear patterns in cryptocurrency volatility, improving prediction accuracy. Its bidirectional structure captures the data's past and future dependencies, providing a more comprehensive analysis. This approach enhances the technique's capability to predict volatility trends with greater reliability.
- The ICPA technique optimizes hyperparameters to improve the model's performance in forecasting cryptocurrency volatility. Refining the search process ensures more precise hyperparameter tuning, improving prediction accuracy. This optimization strengthens the model's capability to adapt to changing market conditions.
- The novelty of the FBLSTMSC-DMPVC method is integrating FBLSTM with ICPA for hyperparameter tuning. This method utilizes the power of fuzzy logic and bidirectional LSTM networks to capture complex patterns in cryptocurrency volatility. This incorporation enhances the model's accuracy by optimizing hyperparameters more effectively through ICPA. By merging these two techniques, the model is better equipped to handle volatile market conditions and deliver more reliable predictions.

Literature survey

Tang et al.¹¹ aim to predict the recognized Bitcoin volatility using an enhanced DL method. Initially, a complete factor indicator method and exploit diverse approaches for feature selection is created, and the random forest (RF)-based feature selection fits proficiently to initiate DL methods. Afterwards, the Particle Swarm Optimization (PSO) method is used to enhance the hyper-parameter of the Gated Recurrent Unit (GRU) method. Amirshahi and Lahmiri¹² created several LSTM and DL methods depending on Feed Forward Neural Networks (DFFNNs) models. Subsequently, dissimilar hybrid methods were made for the 3 GARCH-type outputs, such as EGARCH, APGARCH, and GARCH, with three diverse assumptions for the distribution of the residuals that led to the LSTM and DFFNN models. Specifically, GARCH-type methods were used for feature extraction, and the DL methods leveraged a feature extraction sequence as their inputs to create instability the next day. In¹³, an innovative approach is projected by leveraging probabilistic GRU (P-GRU). This method incorporates probabilistic features into the technique. In search of enhancing method efficiency, a bespoke callback mechanism is employed. This callback mechanism, determined by R2-score tracking, takes optimum method weights depending on the validity of the data. Furthermore, a transfer learning pattern is accepted to extend the investigation's prospects. A pre-trained method on BTC data is connected to forecast values for six other vital cryptocurrencies. Jin and Li¹⁴

implement a new hybrid forecast method, VMD-AGRU-RESVMD-LSTM, that combines the decomposition-incorporation structure with DL methods. The process is initiated by disintegrating the cryptocurrency cost sequence into a limited amount of sub-series, utilizing the Variational Mode Decomposition (VMD) approach. Afterwards, the GRU-NNs are associated with an attention mechanism, individually forecasting every modal element sequence. In addition, the residual sequence is attained after decomposition and endures further decomposition. In¹⁵, a hybrid method that incorporates Bi-LSTM models with FinBERT is presented to improve predicting precision for those properties. This method fills a main gap in predicting unstable economic markets by combining developed time series methods with sentimental analysis, providing valuable points for analysts and investors to navigate changeable markets. In¹⁶, this research's main contribution is using classical DL methods in groups with the three most common ensemble learning models, such as ensemble-bagging, stacking, and averaging, to forecast the major hour values of cryptocurrencies. Classical DL approaches containing a grouping of BiLSTM, convolutional layers, and LSTM were used to evaluate the recommended ensemble approaches.

Ghosh et al.¹⁷ present a granular hybrid predictive modelling structure. Primarily, the main temporal features of the price series are studied. Then, Maximal Overlap Discrete Wavelet Transformation (MODWT) and Ensemble Empirical Mode Decomposition (EEMD) are utilized to disintegrate the unique time series into dual diverse sets of granular subseries. Afterwards, extreme gradient boosting (XGB) and LSTM disintegrate subseries. Finally, Sequential Quadratic Programming (SQP) is utilized to predict by relating the earlier predictions. In¹⁸, a hybrid method is advanced to predict the risk and volatility of economic instruments by relating general econometric GARCH time series methods with DL NNs. GRU models are applied for that final, where four diverse specifications are utilized as the GARCH component. As the significant instability estimator and the fundamental targeted functions of the hybrid methods, this research utilizes the price range-based Garman-Klass estimator, altered to integrate the closing and opening costs. Cho and Lee¹⁹ develop a forecasting model integrating asymmetric fractality and DL to predict one-day-ahead stock price volatility, utilizing asymmetric Hurst exponents and recurrent neural networks (RNNs) for improved performance in volatile markets. Bildirici, Ucan, and Tekercioğlu²⁰ analyze daily and weekly Bitcoin returns utilizing hybrid models, exploring fractal and chaotic structures and comparing the performance of ARFIMA, LieNLS, and LieOLS methods for forecasting. Kabir et al.²¹ propose a novel financial forecasting model, LSTM-mTrans-MLP, integrating LSTM, a modified Transformer, and MLP, showing superior forecasting accuracy, robustness, and sensitivity. Behera, Nayak, and Kumar²² aim to construct optimal ANNs using metaheuristics, namely FWA, CRO, and TLBO, to predict the behaviour of fast-growing cryptocurrencies like Bitcoin, Litecoin, Ethereum, and Ripple. Safari et al.²³ present an ensemble learning approach for portfolio optimization, incorporating ML models such as LSTM, GRU, RF, etc., with mean-variance models using ridge and principal component regression to optimize asset al.locations for balanced risk and return. Nagajothi and Meyyappan²⁴ explore the relationship between public sentiment and Bitcoin price fluctuations utilizing DL fuzzy logic, integrating sentiment data from social media to predict future prices. Rahim et al.²⁵ explore artificial neural networks (ANNs) to develop more advanced trading strategies, addressing the challenges of accurately predicting market patterns and returns in automated trading systems. Koo and Kim²⁶ improve Bitcoin price prediction by introducing the Centralized Clusters Distribution (CCD) for data filtering and the Weighted Empirical Stretching (WES) loss function, enhancing both overall and tail performance using LSTM and SSA decomposition.

The limitations of the existing studies comprise the reliance on single-method approaches for cryptocurrency prediction, which often fail to capture the intrinsic, non-linear relationships in financial markets. While hybrid models show promise, integrating multiple techniques can lead to computational complexity and overfitting. Furthermore, many models do not account for the dynamic nature of cryptocurrencies, which may limit their capability to adapt to sudden market changes. There is also a lack of consistency in evaluating models, as diverse metrics and datasets are often used, making comparisons difficult. Future research should concentrate on improving the adaptability and interpretability of hybrid models while exploring new data sources and methodologies to enhance prediction accuracy.

Materials and methods

In this study, an Empirical Evaluation of the FBLSTMSC-DMPVC technique is presented. The primary focus of the FBLSTMSC-DMPVC technique is to present a robust and intelligent framework for an advanced decision-making model to predict cryptocurrency volatility. To accomplish that, the FBLSTMSC-DMPVC approach has three processes: data normalization, a predicting method using FBLSTM, and ICPA-based parameter tuning. Figure 1 depicts the workflow of the FBLSTMSC-DMPVC approach.

Data normalization

Initially, the presented FBLSTMSC-DMPVC method performs the data preprocessing process using Z-score normalization to ensure all features are standardized and scaled. Z-score normalization is employed to tackle the task set by the distinct measures of the dataset's features²⁷. This technique alters every feature to have a standard deviation of one and a mean of zero, as demonstrated in Eq. (1). This kind of normalization assists the comparison of features with modifying units and scales vital for the successive study.

$$z = \frac{(x - \mu)}{\sigma} \quad (1)$$

Here, where z signifies the value of standardized, x denotes an original value, μ refers to a mean, and σ indicates the standard deviation.

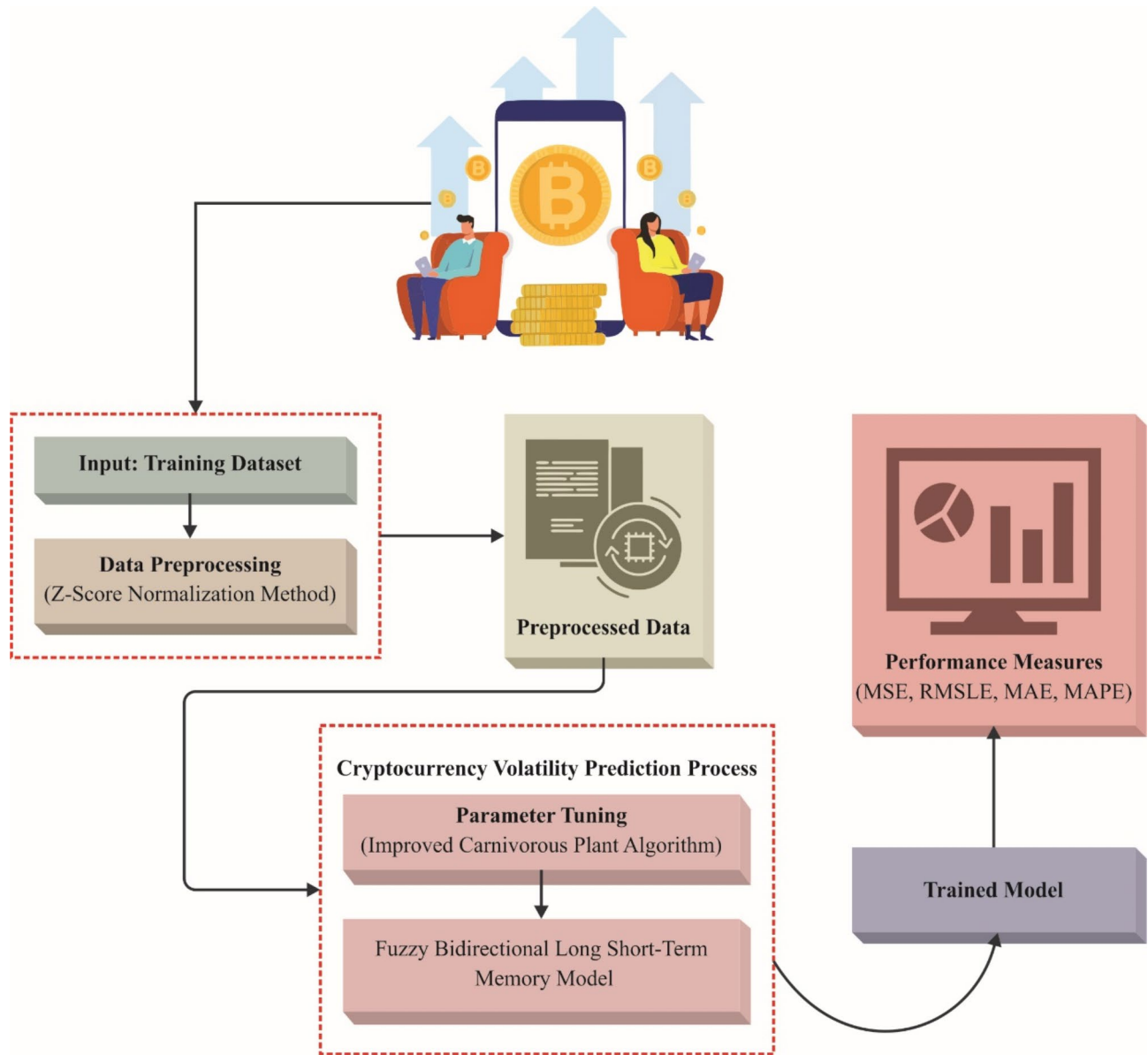


Fig. 1. Workflow of FBLSTMSC-DMPVC approach.

Predicting using the DBLSTM model

Next, the FBLSTM model is employed to predict cryptocurrency volatility. The Bi-LSTM approach is an expansion of the conventional LSTM structure intended to enhance the learning of either future or past context in sequential data²⁸. But standard LSTM models handle data in a direction either backwards (from future to past) or forward (from past to future)-Bi-LSTM methods contain dual layers of LSTM: one handling the sequences in the forward and the other in the backward directions. Incorporating the outputs from either direction requires complete knowledge of the sequences, making it mainly suitable for tasks. It is beneficial to context data from the future or the past. During Bi-LSTM, all input sequences are passed over dual LSTMs:

Both Forward and Backward LSTM Handle the sequences in the traditional left-to-right direction and manage the sequence backwards, from right to left direction. The last hidden layer (HL) at every time step combines the HL from backward or forward LSTMs. This permits the method to utilize data from either direction, enhancing the capability to take longer range dependency, which is lost in unidirectional techniques. This ability is mainly beneficial in tasks like speech recognition, machine translation, and time series prediction, whereas past or future contexts are crucial.

In Mathematics, for every time step t , the LSTM of forward calculates:

$$\vec{h}_t = \text{LSTM} \left(x_t, \vec{h}_{t-1}, \vec{C}_{t-1} \right) \quad (2)$$

However, the LSTM of backward calculates:

$$\overleftarrow{h_t} = LSTM \left(x_t, \overleftarrow{h_{t+1}}, \overleftarrow{C_{t+1}} \right) \quad (3)$$

Whereas x_t refers to input at t th time, $\overleftarrow{h_t}$ and $\overrightarrow{h_t}$ represent HL for the backward and forward LSTMs, and C_{t-1} and C_{t+1} denote states of the cell for all directions. The last HL at every time step t is gained by combining the forward and backward HLs:

$$h_t = \left[\overrightarrow{h_t}; \overleftarrow{h_t} \right] \quad (4)$$

This connected HL has information from either the past or the future, enhancing the method's capability to handle seizure dependency in both directions. Figure 2 exemplifies the structure of BiLSTM.

A fuzzy rule (FR) is a true or false description. During fuzzy logic, inference rules define the values of the output variable according to the input variable's values. Each of the FRs that are successful in fuzzy logic²⁹.

1. Fuzzy control rules

The skills of an expert in some related zone usage must be named the fuzzy control rules. When the controller of the closed-circuit approach has been applied, the FR is considered by a sequence of the category IF-THEN, which results in processes describing which case should be completed in the now specified data that comprises response and input. This rule regulates the construction or design of the group of FR, which is positioned on a human's knowledge or experience that differs based on the particular use. An IF-THEN FR links a condition described by sets of fuzzy and language variables to the outcome. The IF factor is primarily implemented to gather knowledge through elastic conditions; however, the THEN factor is applied to offer an output using the semantical variable method. This inference FR often uses these IF-THEN rules to control the amount to which the input data encounters the state of the rules.

2. Fuzzy mapping rules

It provides effective maps among the input and the output utilizing language variables. It is established based on a fuzzy graph showing the connection between the fuzzy input and output. It may be problematic to remove the particular connection between input and output, or the connection between these inputs and outputs is incredibly intricate even in case it is produced the real-time products. These rules are the right choice for particular cases. Fuzzy mapping rules are equivalent to intuition and human interpretations; each fuzzy mapping rule values a smaller percentage of the function. FR mapping group must be applied to assess the complete functions. The input variables consume numerous sizes in most real-time applications. However, the fuzzy control rules must be extended to consider many inputs; the outputs must be computed.

The inputs differ at a dissimilar step, and these inputs are connected to the IF parts of the rules of IF-THEN. It is recognized as the controller output and 3D variable established at the connection of all rows and columns, and it is connected to the THEN factor of the rules of IF-THEN.

3. Fuzzy implication rules

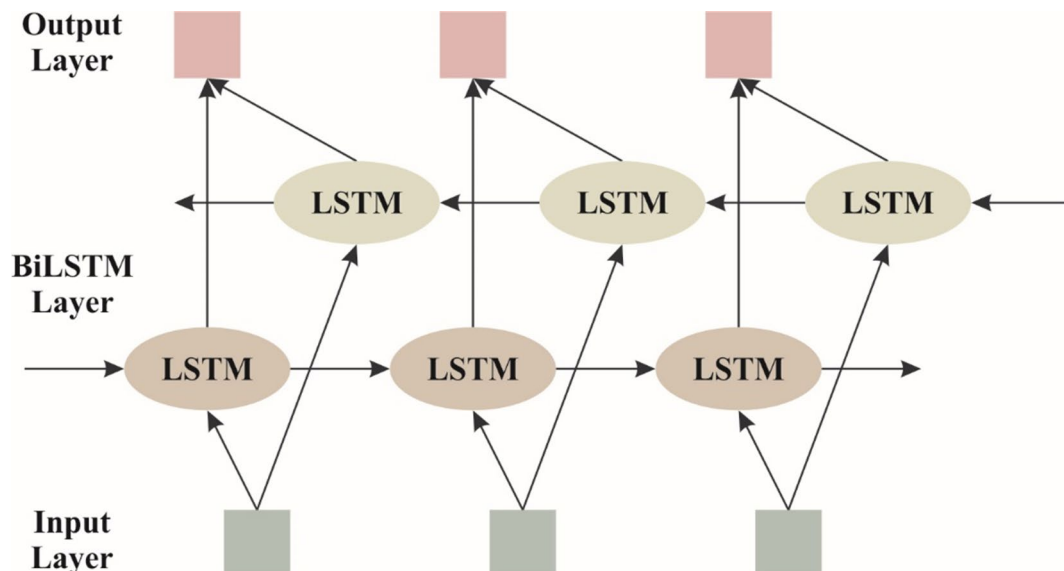


Fig. 2. BiLSTM architecture.

A widespread logic proposes the connection between input and output. A fuzzy implication rule defines it. Every restricted basis of fuzzy logic is the essence of an implication rule of fuzzy. Multi-valued and conventional dualistic logic are associated with the implication rule of fuzzy.

- Similarity Relation—Fuzzification

In comparison with an essential subject for which a basic method is regularly exposed to be inadequate. The measured properties of the fuzzy sets display the insight of the measured properties. The relation of fuzzy equivalence has been applied to exemplify the link between substances of a fuzzy set from the viewpoint of the relation of fuzzy equivalence. Fuzzy sets have been considered to inspire ideas by describing similarity, which is a foundation of the relation of fuzzy equivalence. A fuzzy set can't distinguish dual components when they are members of a similar set or its balance. The group of the membership functions of the fuzzy set utilizing the relation of fuzzy equivalence is described as shown:

- Definition 1

A similarity relation of the fuzzy on set V denotes mapping $E : V \times V \rightarrow [0, 1]$ satisfies

$$(E1) E(v, v) = 1, v \in V \text{ (reflexivity)}$$

$$(E2) E(v_1, v_2) = E(v_2, v_1), v_1, v_2 \in V \text{ (symmetry)}$$

$$(E3) E(v_1, v_2) * E(v_2, v_3) \leq E(v_1, v_3), v_1, v_2, v_3 \in V \text{ (transitivity)}$$

whereas the unit interval is signified as $[0, 1]$ using the standard ordering. Sometimes, E is considered a similarity relation. Consistently, a small number of descriptions and theorems are hereby recollected.

- Definition 2

- A fuzzy set $A \in [0, 1]^u$ is named as extended over the relation of fuzzy equivalence E on V if and only if $\mu_A(v_1) * E(v_1, v_2) \leq \mu_A(v_2)$ carries for each $v_1, v_2 \in V$. Definition 3

Let E represent the fuzzy equivalence relation on V and let $A \in [0, 1]^u$.

The fuzzy set $\hat{A} = \cap \{B \mid A \subseteq B \text{ and } B \text{ are logical about } E\}$ is defined as the relevant hull of A regarding E .

The incorporation of Fuzzy and Bi-LSTM networks, frequently connected with FBLSTM, unites the strengths of both methods to tackle composite problems relating to sequential data and uncertainty. Fuzzy logic is famous for its capability to manage imprecision and vagueness, whereas Bi-LSTM networks perform well in capturing longer-range dependency in sequential data. By joining these two techniques, FBLSTM utilizes fuzzy logic for modelling uncertain inputs and enhances the Bi-LSTM performance in prediction and decision-making tasks. The fuzzy logic module processes uncertain or inaccurate information by changing it into fuzzy sets, which the Bi-LSTM then handles to learn sequential patterns and forecast future states. This combination is valuable in applications such as time series prediction, pattern classification, and speech recognition, whereas either uncertainty or sequential dependencies are essential.

The standard equation for FBLSTM is represented as shown:

$$y_t = BiLSTM(f(x_t, \theta_f)) \quad (5)$$

Whereas, y_t refers to output at t th time step. x_t characterizes the input vector at t th time step. θ_f signifies the fuzzy inference parameters that handle the input over the fuzzy network. $f(x_t, \theta_f)$ represents fuzzy logic conversion used to the input. The Bi-LSTM handles this converted input and outputs the classification or prediction at t .

This equation takes how the fuzzy logic network handles the inputs, and the Bi-LSTM learns the temporal dependency for additional prediction.

Hyperparameter tuning using ICPA

To enhance the hyperparameters of the FBLSTM method, the ICPA is employed^{30,31}. This method is chosen due to its unique search mechanism, which replicates the natural behaviour of carnivorous plants in optimizing solutions. Unlike other techniques such as grid or random search, ICPA can explore a wide search space while averting local optima, making it highly effective for intrinsic, non-convex optimization problems. Its adaptive nature allows it to balance exploration and exploitation, ensuring thorough search and fine-tuning hyperparameters. Furthermore, the capability of the ICPA technique to diversify its search when stuck in local optima provides robustness in finding optimal solutions. Compared to conventional methods, ICPA requires fewer iterations for convergence, mitigating computational costs while improving the quality of hyperparameter tuning. This makes ICPA a more efficient and effective choice for hyperparameter optimization. Figure 3 illustrates the structure of the ICPA model.

To tackle intricate dynamic and kinematic restraints and improve robot guidance routes in multi-objective situations, preceding research work has employed heuristic techniques to classify optimum routes that fulfil third-order restraints. Making these discoveries, an in-depth exploration was conducted, and additional improvements were proposed for a three-dimensional B-spline curve. Notably, the ICPA is presented to enhance the spread of controller point within the cubic B-spline, sustaining third-order restraint needs while improving route efficiency and smoothness. The CPA is a bio-inspired metaheuristic technique that simulates carnivorous plants' existence tactics and variation systems in demanding surroundings. The method establishes higher efficiency in addressing intricate search space issues that are illustrated by higher-dimensional design

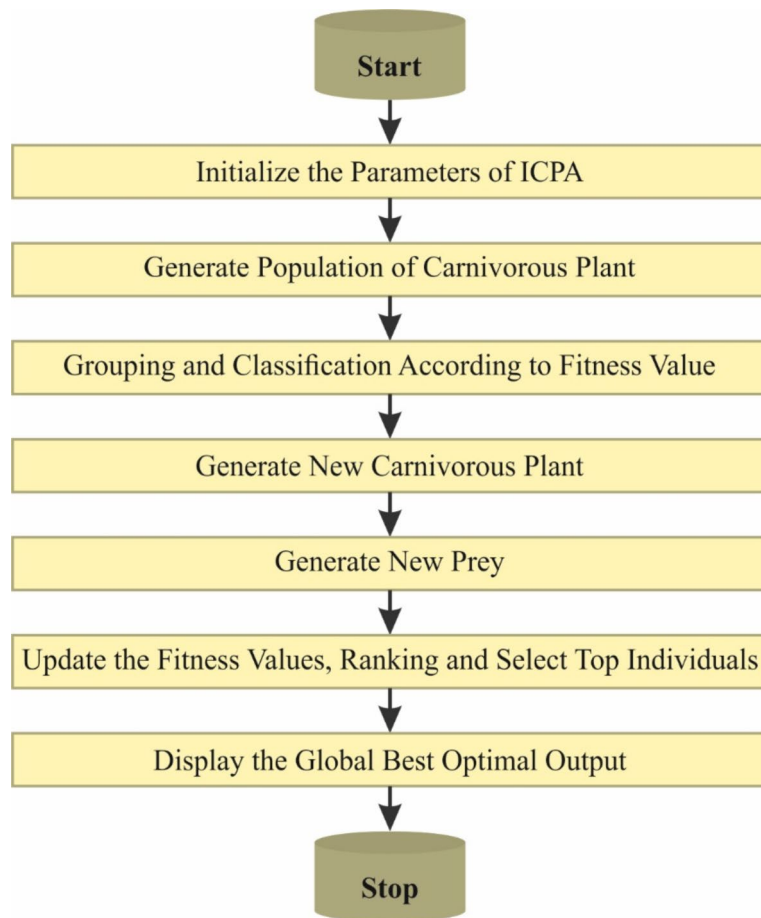


Fig. 3. Steps involved in the ICPA approach.

variables, many restraints, and several local goals. The CPA works through four phases: initialization, grouping, classification, reproduction, and growth.

In the initialization phase, it builds the original population of N individuals, which consists of carnivorous plants (n_{CPlant}) and prey (n_{Prey}), via arbitrary allowance. Notably, n_{Prey} must be k times n_{CPlant} . The longitudinal spread of these individuals was denoted in the form of a matrix.

$$Pop = \begin{bmatrix} X_{1,1} & X_{1,2} & \dots & X_{1,D} \\ X_{2,1} & X_{2,2} & \dots & X_{2,D} \\ \vdots & \vdots & \ddots & \vdots \\ X_{N,1} & X_{N,2} & \dots & X_{N,D} \end{bmatrix} \quad (6)$$

Here, D signifies the dimension and the amount of n_{CPlant} and n_{Prey} equivalents N . The randomly generated initialization of the population follows the below-mentioned formulation:

$$X_{i,j} = L_{b_j} + (U_{b_j} - L_{b_j}) \times rand \quad (7)$$

Assume $i = 1, 2, \dots, N$ and $j = 1, 2, \dots, D$, while U_b and L_b denote the upper and lower limits of the searching area, correspondingly; $rand$ indicates a randomly produced amount in the range of 0 and 1.

During the grouping and classification phase, the technique classifies all individuals in descending order according to their fitness values. Next, it identifies the highest n_{CPlant} individual as a carnivorous plant and the left n_{Prey} Beings as a target. The most appropriate target is allocated to the highest carnivorous plant. Next, the 2nd and 3rd most appropriate prey are set using the consequent carnivorous plant. This procedure continues until every plant is opposite with its consistent prey. Then, the additional prey corresponded again initially with the high-ranking, and the pattern restarted.

In the growth stage, which is a feature of the exploration stage, carnivorous plants issue smells to charm prey. Trapped prey deliver foods that advance plant development; not every prey was well-trapped. To consider this, an attraction rate (ar) was presented, defining the capture of prey by equating the ar value with a randomly generated number between 0 and 1. The formulations employed in this stage are mentioned below:

$$\begin{aligned} NewCP_{i,j} &= growth \times CP_{i,j} + (1 - growth) \times Prey_{v,j} \\ growth &= growth_{rate} \times rand_{i,j} \end{aligned} \quad (8)$$

$$NewPrey_{i,j} = growth \times Prey_{u,j} + (1 - growth) \times Prey_{v,j}, u \neq v$$

$$growth = \begin{cases} growth_rate \times rand_{i,j} & if f(Prey_v) > f(Prey_u) \\ 1 - growth_rate \times rand_{i,j} & if f(Prey_v) < f(Prey_u) \end{cases} \quad (9)$$

While, $CP_{i,j}$ signifies the carnivorous plant of set i , $Prey_{v,j}$ and $Prey_{u,j}$ denote dual randomly chosen preys in set i , respectively; $growth_rate$ refers to a value of pre-defined, $rand_{i,j}$ indicates the randomly produced value within the interval of $[0,1]$.

The reproduction stage observes the commencement of the exploitation method and is repeated depending on the n_{CPlant} value. During this phase, carnivorous plants utilize the foods attained to develop and reproduce, thus making sure that the optimum individuals in the populace, such as the high-rank individuals, are reproduced. This permits the CPA model to concentrate on following the optimum solution.

The calculated representation of the reproduction phase is mentioned below:

$$\begin{aligned} NewCP_{i,j} &= CP_{1,j} + Reproduction_rate \times rand_{i,j} \times mate_{i,j} \\ mate_{i,j} &= \begin{cases} CP_{v,j} - CP_{i,j}, & if f(CP_i) > f(CP_v) \\ CP_{i,j} - CP_{v,j}, & if f(CP_i) < f(CP_v) \end{cases}, \quad i \neq v \neq 1 \end{aligned} \quad (10)$$

Here, $CP_{1,j}$ denotes the finest solution, $CP_{v,j}$ represents a randomly chosen carnivorous plant, and the *reproduction rate* refers to the pre-defined value.

As the number of controller points improves, the searching efficacy of CPA supervises decreases. To tackle this problem, the next developments in the CPA are presented. A chaotic searching tactic has been utilized to enhance the model's primary solution, improving the exploration range. Next, a growth phase tactic depending upon the normal distribution was employed, permitting the technique to actively alter the development direction throughout the search method as per the excellence of the solution. These improvements enhance both the accuracy and efficiency of the exploration. It is denoted as Improved Carnivorous Plant Algorithm (ICPA).

Tent map is a perfect selection for setting the population owing to its efficiency and simplicity in producing a chaotic series. Its mathematical equation is expressed below:

$$x_{n+1} = \begin{cases} \frac{x_n}{0.7}, & 0 < x_n \leq 0.7 \\ \frac{x_n(1-x_n)}{0.3}, & 0.7 < x_n \leq 1 \end{cases} \quad (11)$$

The specific process of utilizing a Tent map is given below:

$$\begin{aligned} X_i^j(0) &= x_{\min} + Chaos \times (x_{\max} - x_{\min}), \\ &\quad \begin{cases} i = 1, 2, \dots, n \\ j = 1, 2, \dots, d \end{cases} \end{aligned} \quad (12)$$

In the equation, $X_i^j(0)$ signifies the first value of i th individual on j th decision variable; x_{\min} and x_{\max} signify the lower and upper limits for independent variables, correspondingly; M represents the number of individuals; d refers to the size of the issue; and *Chaos* indicates the factor of chaos produced over the tent mapping.

People using less objective function values are more likely to resolve the least value during this optimization issue. To help this feature, a novel tactic is presented, in which the progression of off-spring is based upon the typical distribution $N(\mu, \sigma^2)$. Here, μ denotes a chosen parent, and σ refers to a regulating standard deviation, limiting further individuals' search range. As per the 6σ value of the standard distribution, the range of $(\mu - 3\sigma \text{ and } \mu + 3\sigma)$ includes many probable values. By altering σ , the produced off-spring can be focused on μ , thus improving the model's capability to concentrate on the present optimal solution. At the same time, this technique permits the search of novel solutions in an assured span.

To execute this approach, the Eqs above. (8) and (9) are substituted by using novel Eqs. (13) and (14) throughout the off-spring production stage:

$$NewCP_{i,j} = N\left(CP_{i,j}, \sqrt{\varepsilon + \left[\frac{CP_{i,j} - Prey_{v,j}}{6}\right]^2}\right) \quad (13)$$

$$NewPrey_{i,j} = \begin{cases} N\left(CP_{v,j}, \sqrt{\varepsilon + \left[\frac{CP_{i,j} - Prey_{u,j}}{6}\right]^2}\right) & if f(Prey_v) > f(Prey_u) \\ N\left(CP_{u,j}, \sqrt{\varepsilon + \left[\frac{CP_{i,j} - Prey_{v,j}}{6}\right]^2}\right) & if f(Prey_v) < f(Prey_u) \end{cases} \quad (14)$$

Here, ε refers to a small coefficient to guarantee strength and declare a definite measure of randomness.

In this paper, the ICPA has been applied to define the intricate hyperparameter in the FBLSTM approach. The MSE is measured as the objective function and described as shown.

$$MSE = \frac{1}{T} \sum_{j=1}^L \sum_{i=1}^M (y_j^i - d_j^i)^2 \quad (15)$$

Here, L and M consistently characterize the resulting value of layer and data, and y_j^i and d_j^i indicate the achieved and proper magnitudes for the j^{th} component from the resulting layer of the system in t^{th} time, respectively. The pseudocode of the ICPA model is given below.

Initialize population of carnivorous plants (agents)

For each plant i in the population:

 Set initial position xi (solution)

 Set initial fitness value $f(xi)$

Repeat until stopping criteria are met:

 For each plant i in the population:

 Evaluate the fitness $f(xi)$ based on the objective function

 Select neighbouring plants for comparison:

 Select a prey plant j with a higher fitness value than i

 Update the plant i 's position using the prey's position:

$xi = xi + rand() * (xj - xi)$ // Update position towards prey

 If plant i encounters a "trap" (local optimum):

 Diversify plant i 's search:

$xi = xi + rand() * (xmax - xmin)$ // Random repositioning within bounds

 If plant i 's fitness is better than previous:

 Update best position and fitness for i

 Improve hunting behaviour based on the global fitness landscape:

 Randomly adjust hunting strategies of plants for more exploration or exploitation

 If convergence criteria are met (no improvement for several iterations):

 Break

Output best solution found

Pseudocode 1. ICPA Technique

Performance validation

The experimental validation of the FBLSTMSC-DMPVC approach is studied below the Cryptocurrency Price Analysis Dataset³². The major cryptocurrencies are Bitcoin (BTC), Ethereum (ETH), Ripple (XRP), and Litecoin (LTC). The historical volatility is utilized as the measure of volatility, and the data period for analysis spans from January 1, 2018, to May 31, 2023. This timeframe was chosen to represent market conditions and fluctuations during the specified period comprehensively.

Correlation Matrix

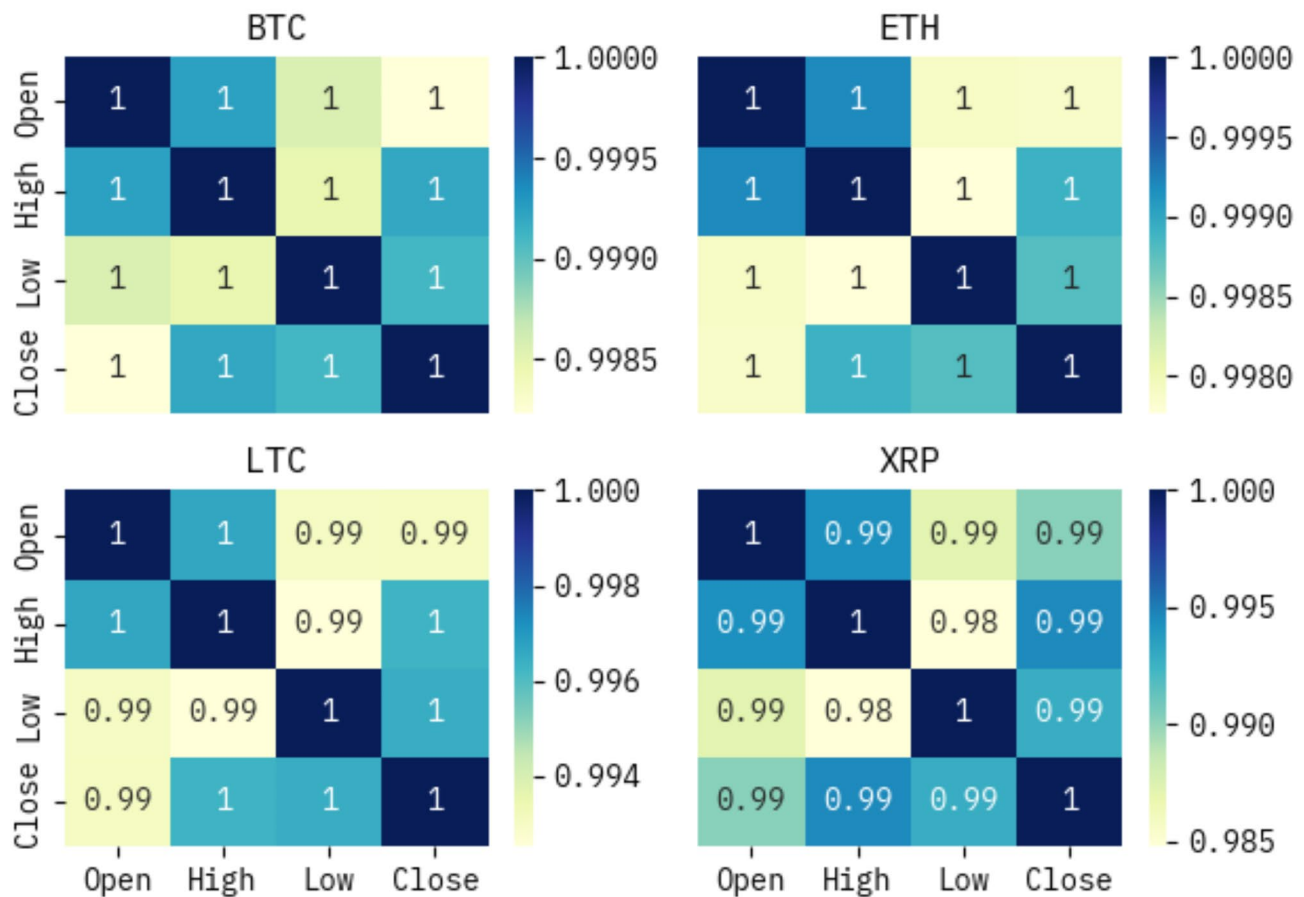


Fig. 4. Correlation matrix of FBLSTMSC-DMPVC model.

Figure 4 establishes the correlation matrix produced by the FBLSTMSC-DMPVC technique. The results identify that the FBLSTMSC-DMPVC model effectively predicts all class labels precisely.

Figure 5 represents the close price result analysis of the FBLSTMSC-DMPVC model under cryptocurrencies.

Figure 6 depicts the pairwise result analysis plot of the FBLSTMSC-DMPVC model for crypto data under different cryptocurrencies.

Figures 7, 8, 9, 10 and 11 shows an outcome analysis graph for the actual vs. prediction of FBLSTMSC-DMPVC methodology under several epochs. The outcomes specified that the FBLSTMSC-DMPVC technique has enhanced prediction results. The figure shows the actual vs. prediction results of the FBLSTMSC-DMPVC approach. The outcomes stated that the FBLSTMSC-DMPVC approaches have exposed better-predicted results under every operation hour. It is also well-known that the variance between the predicted and actual values is measured at the least.

Figure 12 establishes outcome analysis for the loss curve of the FBLSTMSC-DMPVC technique under MAE, MAPE, MSE, and RMSLE. The values of loss are computed over the range of 0–50 epochs. The training values exemplify a diminishing tendency, informing the capacity of the FBLSTMSC-DMPVC methodology to balance a trade-off between data fitting and generalization. The continuous reduction in loss values guarantees the superior performance of the FBLSTMSC-DMPVC methodology and tunes the prediction outcomes over time.

Table 1 provides the classifier result of the FBLSTMSC-DMPVC technique under multiple cryptocurrencies. The table values specify that the BTC cryptocurrency has attained MSE of 0.0015, RMSLE of 0.0369, MAE of 0.0364, and MAPE of 0.7939. At the same time, the ETH cryptocurrency has an MSE of 0.0018, RMSLE of 0.0408, MAE of 0.0423, and MAPE of 0.8633. Meanwhile, LTC cryptocurrency has obtained an MSE of 0.0016, an RMSLE of 0.0351, an MAE of 0.0355, and a MAPE of 0.6187. At last, the XRP cryptocurrency has an MSE of 0.0021, RMSLE of 0.0403, MAE of 0.0414, and MAPE of 0.6667.

Table 2 provides the MSE outcome of the FBLSTMSC-DMPVC technique under various cryptocurrencies with existing models³³. The results indicate that the FBLSTMSC-DMPVC technique performs better. With BTC cryptocurrency, the FBLSTMSC-DMPVC technique has a lesser BTC of 0.0015, unlike the Bi-directional LSTM (Bi-LSTM), LSTM-RNN, Bi-directional GRU (Bi-GRU), Tensor-based Collaborative Fuzzy Spatio-Temporal Model (T-CFSTM), Adaptive Neuro-Fuzzy Inference System (ANCFIS), Linear Regression (LR), Naïve Bayes (NB), Support Vector Machine (SVM), and RF models have obtained greater BTC of 0.0020,

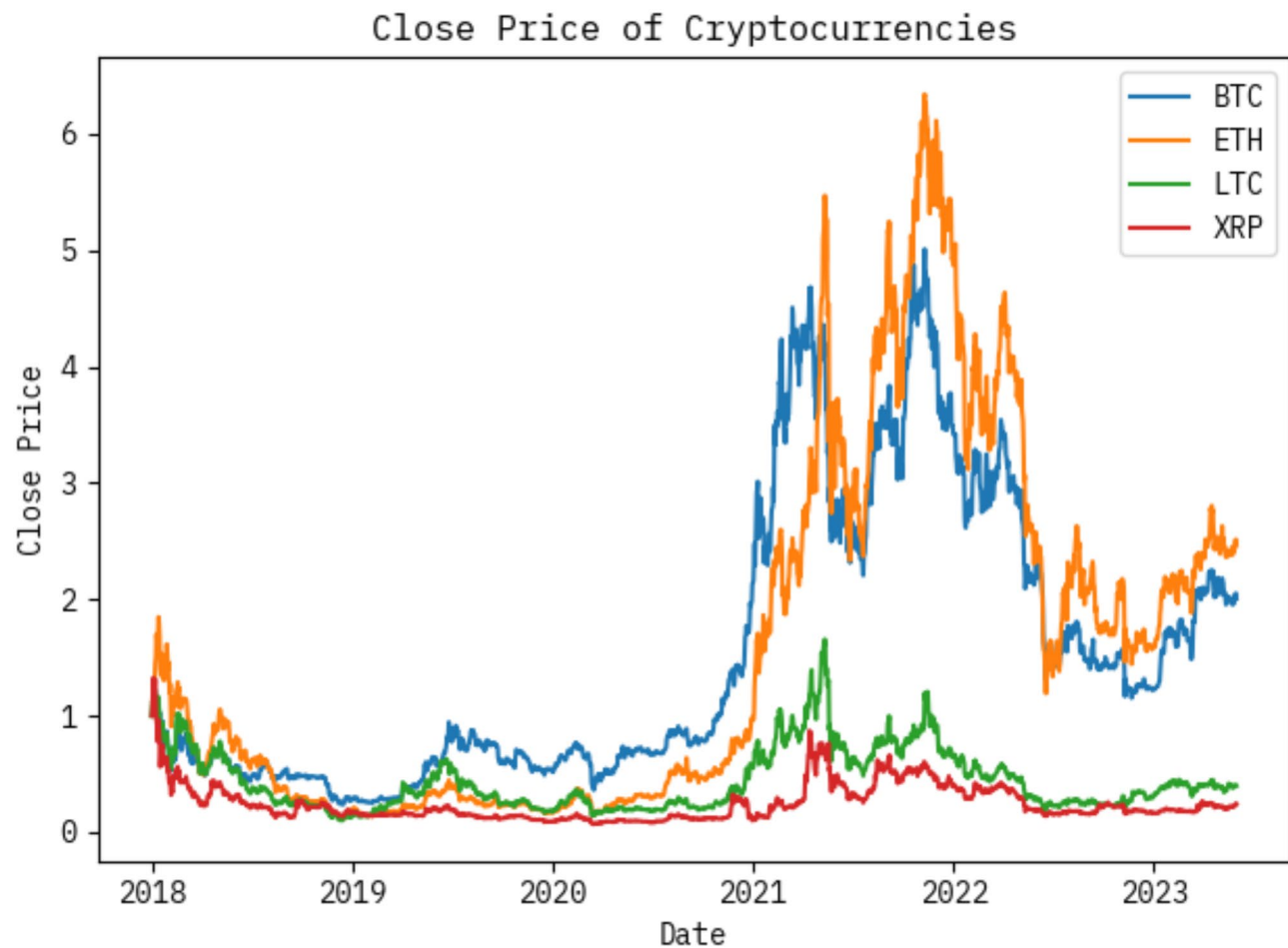


Fig. 5. Close price result analysis of FBLSTMSC-DMPVC model under various cryptocurrencies.

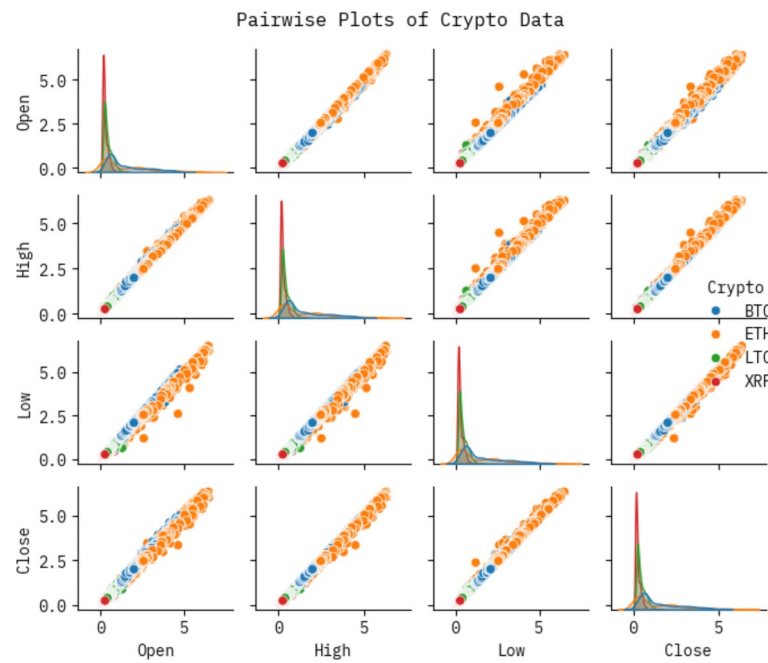


Fig. 6. Pairwise result analysis plot for crypto data.

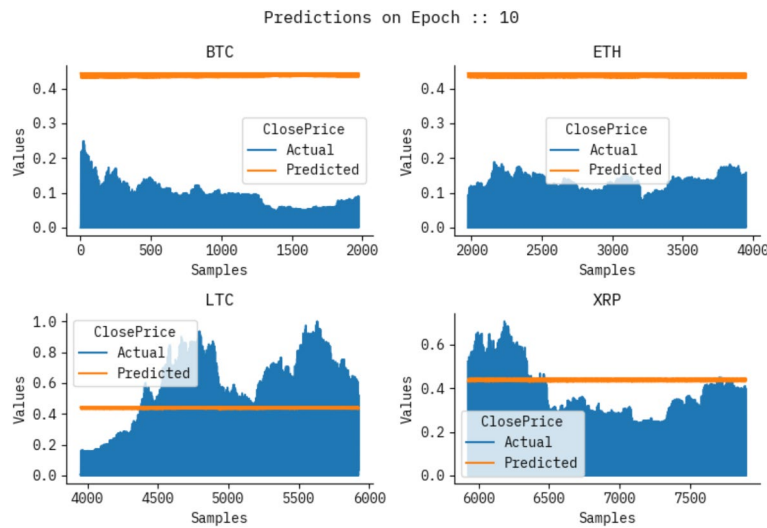


Fig. 7. Result analysis graph of FBLSTMSC-DMPVC model for epoch 10

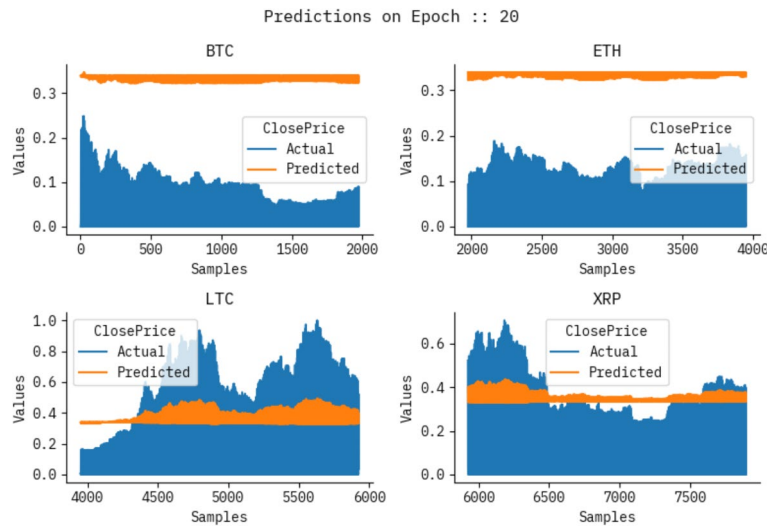


Fig. 8. Result analysis graph of FBLSTMSC-DMPVC model for epoch 20

0.0027, 0.0035, 0.0021, 0.0029, 0.0036, 0.0042, 0.0049, and 0.0057, respectively. Moreover, the FBLSTMSC-DMPVC methodology has gained a lower ETH of 0.0018 with ETH cryptocurrency. In contrast, the Bi-LSTM, LSTM-RNN, Bi-GRU, T-CFSTM, ANCFIS, LR, NB, SVM, and RF methods have achieved superior ETH of 0.0025, 0.0033, 0.0039, 0.0024, 0.0032, 0.0039, 0.0044, 0.0050, and 0.0057, correspondingly. Besides, with LTC cryptocurrency, the FBLSTMSC-DMPVC methodology has attained an inferior LTC of 0.0016. In contrast, the Bi-LSTM, LSTM-RNN, Bi-GRU, T-CFSTM, ANCFIS, LR, NB, SVM, and RF techniques have attained greater LTC of 0.0023, 0.0031, 0.0036, 0.0021, 0.0028, 0.0034, 0.0040, 0.0046, and 0.0054, respectively. At last, with XRP cryptocurrency, the FBLSTMSC-DMPVC methodology has accomplished a minimum XRP of 0.0021. In contrast, the Bi-LSTM, LSTM-RNN, Bi-GRU, T-CFSTM, ANCFIS, LR, NB, SVM, and RF approaches have achieved better XRP of 0.0026, 0.0033, 0.0039, 0.0101, 0.0158, 0.0208, 0.0269, 0.0341, and 0.0400, respectively.

Table 3 presents the MAPE result of the FBLSTMSC-DMPVC method under multiple cryptocurrencies with existing techniques. The outcomes specify that the FBLSTMSC-DMPVC method has higher performance. With BTC cryptocurrency, the FBLSTMSC-DMPVC approach has attained a maximal BTC of 0.7939, whereas the Bi-LSTM, LSTM-RNN, Bi-GRU, T-CFSTM, ANCFIS, LR, NB, SVM, and RF techniques have realized superior BTC of 0.7369, 0.6599, 0.5959, 0.7349, 0.6629, 0.6089, 0.5499, 0.4769, and 0.4019, correspondingly.

With ETH cryptocurrency, the FBLSTMSC-DMPVC methodology has accomplished a maximal ETH of 0.8633. In contrast, the Bi-LSTM, LSTM-RNN, Bi-GRU, T-CFSTM, ANCFIS, LR, NB, SVM, and RF methods have attained greater ETH of 0.8093, 0.7293, 0.6493, 0.8093, 0.7523, 0.6923, 0.6143, 0.5363, and 0.4693, correspondingly. At the same time, With LTC cryptocurrency, the FBLSTMSC-DMPVC model has achieved higher LTC of 0.6187, while the Bi-LSTM, LSTM-RNN, Bi-GRU, T-CFSTM, ANCFIS, LR, NB, SVM, and RF

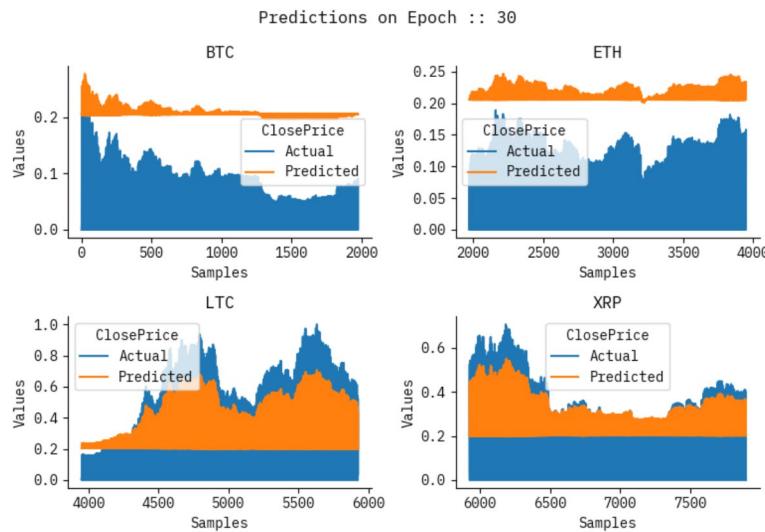


Fig. 9. Result analysis graph of FBLSTMSC-DMPVC model for epoch 30

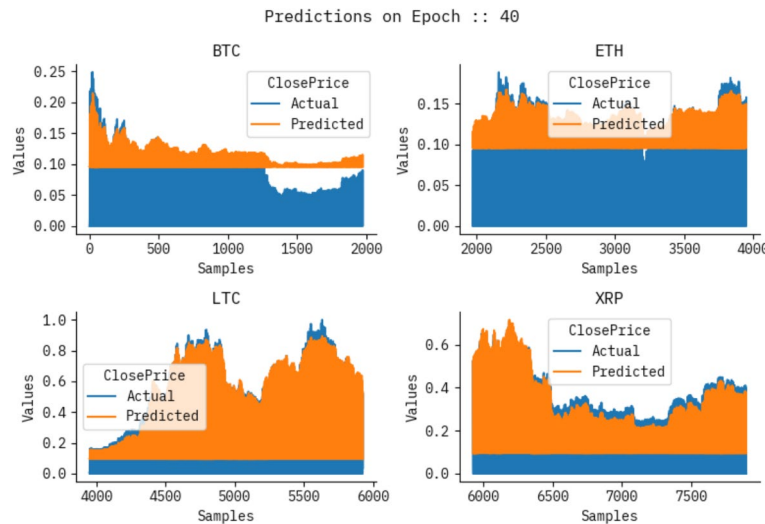


Fig. 10. Result analysis graph of FBLSTMSC-DMPVC model for epoch 40

methods have achieved superior LTC of 0.5437, 0.4927, 0.4157, 0.5457, 0.4757, 0.3977, 0.3377, 0.2677, and 0.1997, individually. Lastly, with XRP cryptocurrency, the FBLSTMSC-DMPVC technique has accomplished a better XRP of 0.6667, whereas the Bi-LSTM, LSTM-RNN, Bi-GRU, T-CFSTM, ANCFIS, LR, NB, SVM, and RF methods have attained greater XRP of 0.5907, 0.5307, 0.4507, 0.5887, 0.5237, 0.4477, 0.3827, 0.3197, and 0.2657, respectively.

Conclusion

In this study, an empirical evaluation of the FBLSTMSC-DMPVC technique is presented. The primary focus of the FBLSTMSC-DMPVC technique is to present a robust and intelligent framework for an advanced decision-making model to predict cryptocurrency volatility. To accomplish that, the FBLSTMSC-DMPVC technique has three processes: normalization, prediction using FBLSTM, and ICPA-based parameter tuning. Initially, the presented FBLSTMSC-DMPVC method performs data preprocessing using Z-score normalization to ensure all features are standardized and scaled. Next, the FBLSTM model is employed to predict cryptocurrency volatility. ICPA is utilized to enhance the hyperparameters of the FBLSTM method. A wide range of simulation is accomplished to ensure the impact of the FBLSTMSC-DMPVC technique. The FBLSTMSC-DMPVC technique portrayed a superior MAPE value of 0.7939 for BTC, 0.8633 for ETH, 0.6187 for LTC, and 0.6667 for XRP, demonstrating its performance across various cryptocurrencies.

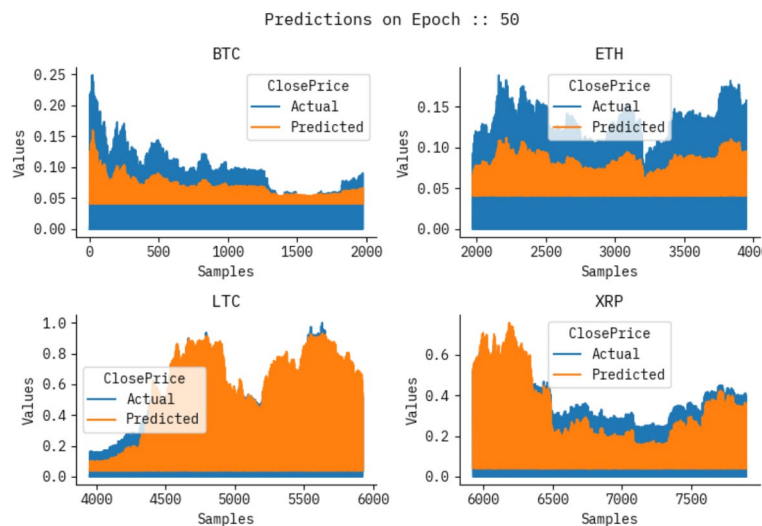


Fig. 11. Result analysis graph of FBLSTMSC-DMPVC model for epoch 50

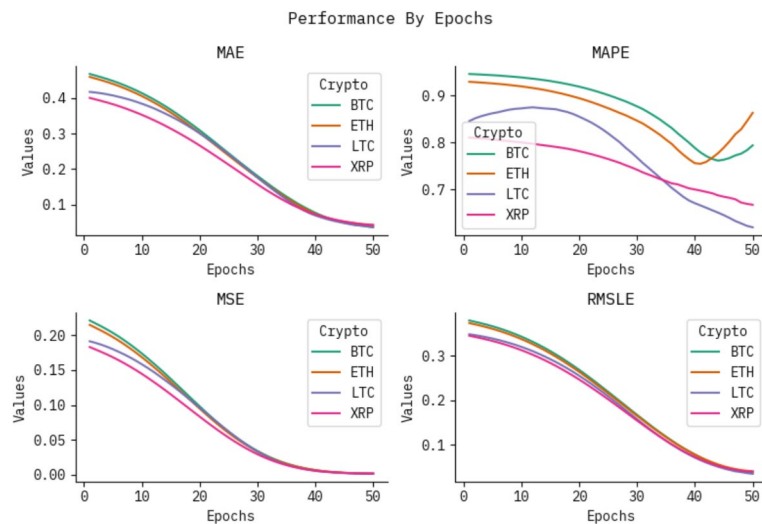


Fig. 12. Result analysis for Loss graph under MAE, MAPE, MSE, RMSLE.

Cryptocurrency	MSE	RMSLE	MAE	MAPE
BTC	0.0015	0.0369	0.0364	0.7939
ETH	0.0018	0.0408	0.0423	0.8633
LTC	0.0016	0.0351	0.0355	0.6187
XRP	0.0021	0.0403	0.0414	0.6667

Table 1. Classifier outcome of FBLSTMSC-DMPVC model under various cryptocurrencies.

MSE				
Algorithm	BTC	ETH	LTC	XRP
FBLSTMSC-DMPVC	0.0015	0.0018	0.0016	0.0021
Bi-LSTM	0.0020	0.0025	0.0023	0.0026
LSTM-RNN	0.0027	0.0033	0.0031	0.0033
Bi-GRU	0.0035	0.0039	0.0036	0.0039
T-CFSTM	0.0021	0.0024	0.0021	0.0101
ANCFIS	0.0029	0.0032	0.0028	0.0158
LR	0.0036	0.0039	0.0034	0.0208
NB	0.0042	0.0044	0.0040	0.0269
SVM Method	0.0049	0.0050	0.0046	0.0341
RF	0.0057	0.0057	0.0054	0.0400

Table 2. MSE outcome of FBLSTMSC-DMPVC technique under existing models under various cryptocurrencies.

MAPE				
Algorithm	BTC	ETH	LTC	XRP
FBLSTMSC-DMPVC	0.7939	0.8633	0.6187	0.6667
Bi-LSTM	0.7369	0.8093	0.5437	0.5907
LSTM-RNN	0.6599	0.7293	0.4927	0.5307
Bi-GRU	0.5959	0.6493	0.4157	0.4507
T-CFSTM	0.7349	0.8093	0.5457	0.5887
ANCFIS	0.6629	0.7523	0.4757	0.5237
LR	0.6089	0.6923	0.3977	0.4477
NB	0.5499	0.6143	0.3377	0.3827
SVM Method	0.4769	0.5363	0.2677	0.3197
RF	0.4019	0.4693	0.1997	0.2657

Table 3. MAPE outcome of FBLSTMSC-DMPVC technique with existing models under various cryptocurrencies.

Data availability

The data that support the findings of this study are openly available in Kaggle repository at <https://www.kaggle.com/datasets/adityamhaske/cryptocurrency-price-analysis-dataset>, reference number³².

Received: 20 December 2024; Accepted: 5 March 2025

Published online: 12 March 2025

References

1. Karim, F., Majumdar, S., Darabi, H. & Harford, S. Multivariate LSTM-FCNS for time series classification. *Neural Netw.* **116**(2), 237–245 (2019).
2. Ergen, T. & Kozat, S. S. Unsupervised anomaly detection with LSTM neural networks. *IEEE Trans. Neural Netw. Learn. Syst.* **31**(8), 3127–3141 (2019).
3. Bacanin, N. et al. Multivariate energy forecasting via metaheuristic tuned long-short term memory and gated recurrent unit neural networks. *Inf. Sci.* **642**, 119122 (2023).
4. Huang, C., Karimi, H. R., Mei, P., Yang, D. & Shi, Q. Evolving long short-term memory neural network for wind speed forecasting. *Inf. Sci.* **632**(20), 390–410 (2023).
5. Lindemann, B., Maschler, B., Sahlab, N. & Weyrich, M. A survey on anomaly detection for technical systems using LSTM networks. *Comput. Ind.* **131**, 103498.
6. Aras, S. Stacking hybrid GARCH models for forecasting bitcoin volatility. *Expert Syst. Appl.* **174** (2021).
7. Jabor, F. K., Al-Attar, B., Naffakh, H. A. & Tawfeq, J. F. H.A. and Implementation of novel cryptographic technique for enhancing the cipher security for resilient infrastructure. *Fusion Pract. Appl.* **15**(1) (2024).
8. D'Amato, V., Levantesi, S. & Piscopo, G. Deep learning in predicting cryptocurrency volatility. *Phys. A Stat. Mech. Appl.* **596** (2022).
9. Li, P., Gu, H., Yin, L. & Li, B. Research on trend prediction of component stock in fuzzy time series based on deep forest. *CAAI Trans. Intell. Technol.* **7**(4), 617–626 (2022).
10. Abdel-Basset, M. & Elhoseny, M. Intelligent feature subset selection with machine learning based risk management for DAS prediction. *J. Cybersecur. Inform. Manag.* (2021).
11. Tang, X., Song, Y., Jiao, X. & Sun, Y. On forecasting realized volatility for bitcoin based on deep learning PSO-GRU model. *Comput. Econ.* **63**(5), 2011–2033 (2024).
12. Amirshahi, B. & Lahmiri, S. Hybrid deep learning and GARCH-family models for forecasting volatility of cryptocurrencies. *Mach. Learn. Appl.* **12**, 100465 (2023).
13. Golnari, A., Komeili, M. H. & Azizi, Z. Probabilistic deep learning and transfer learning for robust cryptocurrency price prediction. *Expert Syst. Appl.* **124404** (2024).

14. Jin, C. & Li, Y. Cryptocurrency Price Prediction Using Frequency Decomposition and Deep Learning. *Fractal Fract.* **7**(10), 708 (2023).
15. Hossain, M. F. B., Lamia, L. Z., Rahman, M. M. & Khan, M. M. FinBERT-BiLSTM: A deep learning model for predicting volatile cryptocurrency market prices using market sentiment dynamics. arXiv preprint <https://arxiv.org/abs/2411.12748> (2024).
16. Rao, K. R. et al. Time-series cryptocurrency forecasting using ensemble deep learning. In *2023 International Conference on Circuit Power and Computing Technologies (ICCPCT)* 1446–1451 (IEEE, 2023).
17. Ghosh, I., Jana, R. K. & Sharma, D. K. A novel granular decomposition based predictive modeling framework for cryptocurrencies' prices forecasting. *China Finance Rev. Int.* (2024).
18. Michański, J., Kwiatkowski, L. & Morajda, J. Combining Deep Learning and GARCH Models for Financial Volatility and Risk Forecasting. arXiv preprint <https://arxiv.org/abs/2310.01063> (2023).
19. Cho, P. & Lee, M. Forecasting the volatility of the stock index with deep learning using asymmetric Hurst exponents. *Fractal Fract.* **6**(7), 394 (2022).
20. Bildirici, M., Ucan, Y. & Tekercioglu, R. A hybrid approach combining the lie method and long short-term memory (LSTM) network for predicting the bitcoin return. *Fractal Fract.* **8**(7), 413 (2024).
21. Kabir, M. R., Bhadra, D., Ridoy, M. & Milanova, M. LSTM-transformer-based robust hybrid deep learning model for financial time series forecasting. *Science* **7**(1), 7 (2025).
22. Behera, S., Nayak, S. C. & Kumar, A. P. Evaluating the performance of metaheuristic based artificial neural networks for cryptocurrency forecasting. *Comput. Econ.* **64**(2), 1219–1258 (2024).
23. Safari, M., Nakharutai, N., Chiawkhun, P. & Phetpradap, P. Mean–Variance Portfolio Optimization Using Ensemble Learning-Based Cryptocurrency Price Prediction (2025).
24. Nagajothi, N. & Meyyappan, T. Bitcoin price prediction using deep learning and fuzzy logic. In *2024 5th International Conference on Electronics and Sustainable Communication Systems (ICESC)* 1330–1337 (IEEE, 2024).
25. Rahim, M. A. et al. Technical analysis-based unsupervised intraday trading Djia index stocks: Is it profitable in long term? *Appl. Intell.* **55**(2), 1–12 (2025).
26. Koo, E. & Kim, G. Centralized decomposition approach in LSTM for Bitcoin price prediction. *Expert Syst. Appl.* **237**, 121401 (2024).
27. Sarmas, E., Fragkiadaki, A. & Marinakis, V. Explainable AI-based ensemble clustering for load profiling and demand response. *Energies* **17**(22), 5559 (2024).
28. Praveenkumar, A., Jha, G. K., Madival, S. D., Lama, A. & Kumar, R. R. Deep learning approaches for potato price forecasting: comparative analysis of LSTM, Bi-LSTM, and AM-LSTM models. *Potato Res.* 1–23 (2024).
29. Alattab, A. A., Ibrahim, M. E., Irshad, R. R., Yahya, A. A. & Al-Awady, A. A. Fuzzy-HLSTM (Hierarchical long Short-Term Memory) for agricultural based information mining. *CMC Comput. Mater. Contin.* **74**(2), 2397–2413 (2023).
30. Wei, B. et al. Smooth and time-optimal trajectory planning for robots using improved carnivorous plant algorithm. *Machines* **12**(11), 802 (2024).
31. <https://www.kaggle.com/datasets/adityamhaske/cryptocurrency-price-analysis-dataset>.
32. Thong, N. T., Quyet, N. V., Giap, C. N., Giang, N. L. & Lan, L. T. H. A complex fuzzy LSTM network for Temporal-Related forecasting problems. *Comput. Mater. Contin.* **80**(3) (2024).
33. Mouiche, I. & Saad, S. Entity and relation extractions for threat intelligence knowledge graphs. *Comput. Secur.* **148**, 104120 (2025).

Acknowledgements

This Project was funded by the KAU Endowment (WAQF) at King Abdulaziz University (KAU), Jeddah, Saudi Arabia, under grant no. (WAQF: 175-611-2024). The author, therefore, acknowledges with thanks WAQF and the Deanship of Scientific Research (DSR) for technical and financial support.

Author contributions

M.R.: Conceptualization, Data curation, Formal analysis, Methodology, Funding Support, Project administration and Resources, Validation and Visualization, Writing—original draft, Writing—review and editing.

Declarations

Competing interests

The author declares no competing interests.

Ethics approval

This article does not contain any studies with human participants performed by any of the authors.

Additional information

Correspondence and requests for materials should be addressed to M.R.

Reprints and permissions information is available at www.nature.com/reprints.

Publisher's note Springer Nature remains neutral with regard to jurisdictional claims in published maps and institutional affiliations.

Open Access This article is licensed under a Creative Commons Attribution-NonCommercial-NoDerivatives 4.0 International License, which permits any non-commercial use, sharing, distribution and reproduction in any medium or format, as long as you give appropriate credit to the original author(s) and the source, provide a link to the Creative Commons licence, and indicate if you modified the licensed material. You do not have permission under this licence to share adapted material derived from this article or parts of it. The images or other third party material in this article are included in the article's Creative Commons licence, unless indicated otherwise in a credit line to the material. If material is not included in the article's Creative Commons licence and your intended use is not permitted by statutory regulation or exceeds the permitted use, you will need to obtain permission directly from the copyright holder. To view a copy of this licence, visit <http://creativecommons.org/licenses/by-nc-nd/4.0/>.

© The Author(s) 2025